Федеральное государственное автономное образовательное учреждение высшего образования “Московский физико-технический институт (национальный исследовательский университет)”

На правах рукописи

Элнаггар Мохамед Мохамед Рагаб

РАЗРАБОТКА НОВЫХ ЭЛЕКТРОН-ТРАНСПОРТНЫХ МАТЕРИАЛОВ ДЛЯ ВЫСОКОЭФФЕКТИВНЫХ И СТАБИЛЬНЫХ ПЕРОВСКИТНЫХ СОЛНЕЧНЫХ БАТАРЕЙ

Специальность 01.04.17 —

«Химическая физика, горение и взрыв, физика экстремальных состояний вещества»

АВТОРЕФЕРАТ

диссертации на соискание ученой степени

кандидата физико-математических наук

Научный руководитель:

кандидат химических наук

Трошин Павел Анатольевич

Москва — 2021

Работа выполнена на кафедре физики организованных структур и химических процессов МФТИ; эта кафедра является базовой кафедрой в ИПХФ РАН (Институт проблем химической физики РАН).

Научный руководитель: кандидат химических наук,

Трошин Павел Анатольевич

Ведущая организация: Федеральное государственное автономное образовательное учреждение высшего образования «Уральский федеральный университет имени первого Президента России Б.Н. Ельцина»

Защита состоится «__» августа 2021 г. в _____ на заседании диссертационного совета _____ по адресу: 141701, Московская область, г. Долгопрудный, Институтский переулок, д. 9, МФТИ.

С диссертацией можно ознакомиться в библиотеке и на сайте Федерального государственного автономного образовательного учреждения высшего образования «Московский физико-технический институт (национальный исследовательский университет)» https://mipt.ru/education/post-graduate/soiskateli-fiziko-matematicheskie-nauki.php

Работа представлена _____ 2021 г. в Аттестационную комиссию федерального государственного автономного образовательного учреждения высшего образования «Московский физико-технический институт» (национальный исследовательский университет) для рассмотрения советом по защите диссертаций на соискание учёной степени кандидата наук в соответствии с п. 3.1 ст. 4 Федерального закона «О науке и государственной научно-технической политике».

Moscow Institute of Physics and Technology

(National Research University-MIPT)

Manuscript

Mohamed Mohamed Ragab Elnaggar

DEVELOPMENT OF NEW ELECTRON-TRANSPORT MATERIALS FOR HIGHLY EFFICIENT AND STABLE PEROVSKITE SOLAR CELLS

Synopsis

dissertation for the degree of

candidate of physical and mathematical sciences

Scientific Supervisor

Pavel A. Troshin

Moscow – 2021

The work has been performed at the Department of Physics of Organized Structures and Chemical Processes of the Moscow Institute of Physics and Technology; this department is the base department at the IPCP RAS (Institute of Problems of Chemical Physics of the Russian Academy of Sciences).

Scientific supervisor: PhD in Chemistry,

Pavel A. Troshin

The defense of the dissertation will be held on «____» August 2021 at ____, at the meeting of the dissertation council _____, at 141701, Moscow region, Dolgoprudniy, Institutskiy per., 9, MIPT.

The dissertation is stored in the library and published on the site of Moscow Institute of Physics and Technology (national research university). https://mipt.ru/education/post-graduate/soiskateli-fiziko-matematicheskie-nauki.php

The work was submitted on _____ to the Attestation Commission of the Moscow Institute of Physics and Technology (National Research University) for consideration by the council for the defense of dissertations for the degree of candidate of science, doctor of science in accordance with paragraph 3.1 Art. 4 of the Federal Law «On Science and State scientific and technical policy».

General description of the subject of work

Hybrid perovskite solar cells (PSCs) have shown a rapid increase in the solar light power conversion efficiency (PCE) within the last few years surpassing recently the 25.5 % threshold and coming close to the crystalline silicon photovoltaics. However, the progress in improving the stability of PSCs is far from being satisfactory, and therefore, short operational lifetimes represent the main obstacle for the successful commercialization of perovskite photovoltaic technology. Decay in the efficiency of completed p-i-n or n-i-p PSC architectures under light exposure can be caused by tens of different factors. Even when the experiments are performed under an inert atmosphere, which excludes the impact of extrinsic factors, such as oxygen and moisture, the device failure can be induced by degradation of the absorber layer, HTL or ETL materials, absorber/HTL and absorber/ETL interfaces, and interfaces between the charge-transport materials and the electrodes. As such, this thesis is dedicated to the development of advanced electron transport layers (ETLs) for p–i-n perovskite solar cells. ETL is an essential component of PSCs and is responsible for the collection of photogenerated electrons. Optimal ETLs should be chemically inert with respect to the complex lead halides, have minimized LUMO energy level offsets with the conduction band of the absorber material, enable efficient and selective extraction of charge carriers, and provide good isolation of perovskite layer, thus preventing its decomposition. Therefore, we tried to fill this gap by exploring a family of new fullerene derivatives, conjugated polymers, and metal oxides as promising ETL materials for p-i-n PSCs.

The Objectives of the Thesis

1. Investigation of the interfacial degradation effects in p-i-n perovskite solar cells. Developing the methodology for decoupling the contributions of the electron- and hole-transport layers to the overall device aging kinetics.

2. A systematic study of a series of functional fullerene derivatives as promising electron transport materials for p-i-n perovskite solar cells. Search for correlations between the material structure and device electrical performance and stability.

3. Investigation of n-type conjugated oligomers and polymers as well as their combinations with fullerene derivatives as electron-transport materials for perovskite solar cells with improved stability.

4. Design and investigation of the metal oxide-based electron transport materials for efficient and stable p-i-n perovskite solar cells.

Scientific Novelty

We have developed an efficient methodology for the investigation of interface degradation effects in p-i-n PSCs and decoupling the contributions of ETL/perovskite and perovskite/ HTL junctions to the overall device aging kinetics. Furthermore, we performed a systematic study and introduced a family of fullerene derivatives, conjugated oligomers or polymers, and metal oxides as advanced ETL materials providing high efficiency and largely improved operational stability of p-i-n PSCs. The results presented in the thesis are expected

to contribute significantly to the development of perovskite solar cells with long operational lifetimes required for their commercial application.

The Theoretical and Practical Value of the Work in the Thesis

The utilization of clean and renewable energy sources has become a prerequisite for the development of human society. Among a variety of new energy technologies, perovskite solar cells are undoubtedly one of the most promising technologies. Hybrid perovskite solar cells (PSCs) have demonstrated impressive efficiencies going beyond 25%, whereas short operational lifetimes represent the main obstacle for their successful commercialization. This problem can be potentially solved by rational engineering of all the perovskite solar cell components, in particular the electron transport layer. Therefore, we focused in this thesis on the exploration of a family of new fullerene derivatives, conjugated oligomers or polymers, and metal oxides as ETL materials for p-i-n PSCs. The most promising electron transport materials for p-i-n devices were identified and the potential for further stability improvement was outlined, thus leading to increased operation lifetimes of perovskite photovoltaics.

Statements to Be Defended

The statements to be defended in the thesis can be enumerated as follows:

1. An efficient methodology was developed for the investigation of interface degradation effects in p-i-n perovskite solar cells (PSCs). The proposed approach allows one to decouple the contributions of ETL/perovskite and perovskite/HTL interfaces to the overall device aging kinetics.

2. A series of structurally similar fullerene derivatives were systematically studied as electron transport layer materials for p-i-n PSCs. It was shown that even a minor modification of the molecular structure of the fullerene derivatives has a strong impact on their electrical performance and, particularly, the ambient stability of the devices. Indeed, an optimally functionalized fullerene derivative applied as an ETL enables stable operation of perovskite solar cells when exposed to air for >800 h, which is manifested in retention of 90% of the original photovoltaic performance.

3. A novel pyrrolo[3,4-c]pyrrole-1,4-dione-based n-type conjugated polymer was introduced as an electron transport material for perovskite solar cells. Blending this polymer with the fullerene derivative $PC_{61}BM$ delivered a decent power conversion efficiency of 16.4% in p-i-n perovskite solar cells using methylammonium-free $Cs_{0.12}FA_{0.88}PbI_3$ absorber in combination with the largely improved operational stability of the devices.

4. Alternating oligomeric compounds TBTBT (“T” - thiophene, “B” - benzothiadiazole) and F4TBTBT were studied as electron transport materials in p-i-n PSCs. The fabricated devices demonstrated a decent power conversion efficiency (PCE) of 10.5%, which was improved to 17.8% by inserting a thin $PC_{61}BM$ interlayer between the perovskite absorber layer and TBTBT-based ETL. The implementation of TBTBT as ETL enhanced the operational stability of perovskite solar cells as compared to the reference devices using the conventional fullerene derivative $PC_{61}BM$.

5. Tungsten oxide (WO_X) was integrated for the first time as electron-transport material for p-i-n PSCs. We have achieved a high device efficiency of up to 18.4% in combination with the record-breaking operational stability of PSCs under continuous light illumination at a high temperature of 60 ºC. The $MAPbI_3$-based devices with WO_X used as electron-transport layer retained ~70% of their initial performance after 4600 h at such harsh aging conditions, whereas the reference cells assembled with $PC_{61}BM$ ETL degraded completely within 50 h.

Presentations and Validation of Research Results

The results of the thesis were reported and discussed at the following scientific conferences and seminars:

1. **M. Elnaggar**, M. Elshobaki, S. Tsarev, K. J. Stevenson, Y. S.Fedotov, S. I. Bredikhin, P. A. Troshin. Skoltech and MIT conference "Collaborative Solutions for Next Generation Education, Science and Technology". Skolkovo Innovation Center, Moscow (**2018**).
2. **M. Elnaggar**, M. Elshobaki, S. Tsarev, K. J. Stevenson, Y. S.Fedotov, S. I. Bredikhin, P. A. Troshin. The 2019 Spring Meeting of the European Materials Research Society (E-MRS), 27-31 May **2019**, Nice, France.
3. **M. Elnaggar**, A. G. Boldyreva, M. Elshobaki, S. A. Tsarev, Y. S. Fedotov, O. R. Yamilova, S. I. Bredikhin, K. J. Stevenson, S. M. Aldoshin and P. A. Troshin. The 1st International School on Hybrid, Organic and Perovskite Photovoltaics (HOPE-PV 2019), October 21-23, **2019**, Moscow.
4. **M. Elnaggar**, A. G. Boldyreva, M. Elshobaki, S. A. Tsarev, Y. S. Fedotov, O. R. Yamilova, S. I. Bredikhin, K. J. Stevenson, S. M. Aldoshin and P. A. Troshin. Methods to analyze stability of perovskite-type absorbers and solar cells (nanoGe Online Meetup Conference), 2-3 June, **2020**. https://www.nanoge.org/StabPero/home
5. **M. Elnaggar**, I, E. Kuznetsov, A. V. Akkuratov, P. A. Troshin. Moscow Autumn Perovskite Photovoltaics International Conference (MAPPIC-2020), 26-28 October, **2020**.
6. **M. Elnaggar**, I, E. Kuznetsov, A. V. Akkuratov, P. A. Troshin. The 2nd School on Hybrid, Organic and Perovskite Photovoltaics (HOPE-PV2020), 3-5 November, **2020**.

List of Publications

This doctoral dissertation consists of a summary of the following publications:

1.**M. Elnaggar**, M. Elshobaki, A. Mumyatov, S. Yu. Luchkin, K. J. Stevenson, P. A. Troshin, Molecular engineering of the fullerene-based electron transport layer materials for improving ambient stability of perovskite solar cells. RRL Solar, **2019**, 3, 1900223. **https://doi.org/10.1002/solr.201900223**

2. A. G. Boldyreva, A. F. Akbulatov, **M. Elnaggar**, S. Yu. Luchkin, A. V. Danilov, I. S. Zhidkov, O. R. Yamilova, Yu. S. Fedotov, S. I. Bredikhin, E. Z. Kurmaev, K. J. Stevenson, and P. A. Troshin. Impact of charge transport layers on photochemical stability of $MAPbI_3$ in thin films and perovskite solar cells, Sustainable Energy Fuels, **2019**, 3, 2705-2716. https://doi.org/10.1039/C9SE00493A

3.**M. Elnaggar**, A. G. Boldyreva, M. Elshobaki, S. A. Tsarev, Y. S. Fedotov, O. R. Yamilova, S. I. Bredikhin, K. J. Stevenson, S. M. Aldoshin and P. A. Troshin. Decoupling Contributions of Charge-Transport Interlayers to Light-Induced Degradation of p-i-n Perovskite Solar Cells. RRL Solar, **2020**, 4, 2000191. **https://doi.org/10.1002/solr.202000191**

4. **M. Elnaggar**, A. M. Gordeeva, A. V. Akkuratov, S. Yu. Luchkin, S. A. Tsarev, K. J. Stevenson, S. M. Aldoshin, P. A. Troshin. Improving Stability of Perovskite Solar Cells Using Fullerene-Polymer Composite Electron Transport Layer. Submitted, **2021**.

5. **M. Elnaggar**, S. M. Aldoshin, P. A. Troshin. Alternating Thiophene-Benzothiadiazole Oligomer as Electron Transport Material for Inverted Perovskite Solar Cells. Submitted, **2021**.

6. **M. Elnaggar**, S. M. Aldoshin, P. A. Troshin et al., Using Tungsten Oxide as ETL Material Enables High Efficiency and Long-Term Operational Stability of p-i-n Perovskite Solar Cells. Submitted, **2021**.

Author's Contribution

The author performed the major part of the research presented in papers (1), (3), (4), (5), (6), and (7). The author participated in the design and personally conducted all the experiments, fabricated and characterized the devices, and analyzed the experimental data. The author was responsible for writing the original draft of each paper. The author in the 2nd paper fabricated and characterized the devices in the following configuration: ITO/PTAA/$MAPbI_3$/$PC_{61}BM$/Mg/Ag. Mr. A. Mumyatov synthesized and provided a new set of fullerene derivatives reported in the 1st and 7th papers. Dr. A. G. Boldyreva prepared the ITO/PTAA/perovskite and ITO/NiO_x/perovskite samples for ToF-SIMS analysis in the 3rd paper. In th 4th paper, Mrs. M. Gordeeva and Dr. A. V. Akkuratov synthesized the new polymer (P1). In 5th paper, the TBTBT and F4TBTBT materials were provided by Dr. A. Akkuratov and Mr. I. Kuznetsov. Dr. Lyubov A. Frolova, Dr. Nadezhda Dremova, Dr. Sergey. Yu. Luchkin, Dr. Sergey A. Tsarev, Dr. Yury Fedotov, Mrs. Marina Utiniva supported this work with the SEM, AFM, PL, ToF SIMS and contact angle measurements.

The structure and amount of the thesis.

The thesis consists of an abstract, five chapters and a list of 176 references.
The full volume of the dissertation is 110 pages, including 53 figures and 9 tables.

The content of the work

The abstract gives a brief description of the whole dissertation and defines the purpose of each section.

The 1st chapter emphasizes the impact of the research conducted within the framework of the thesis, provides an overview of the scientific literature on the problem under study and a summary of each chapter in the thesis, outlines the goal and objectives of the thesis, and evaluates the scientific novelty, theoretical and practical value of the presented thesis.

The 2nd chapter is entitled "Decoupling Contributions of Charge-Transport Interlayers to Light-Induced Degradation of p i-n Perovskite Solar Cells". This chapter is dedicated to the efficient methodology developed for the investigation of interface degradation effects in p-i-n perovskite solar cells (PSCs).

We performed a systematic and comparative study of the aging effects induced by the benchmark electron-transport material $PC_{61}BM$ and three frequently used model HTL materials: PEDOT:PSS, NiO_x, PTAA (poly[bis(4-phenyl)(2,4,6-trimethylphenyl)amine]) and hybrid NiO_x/PTAA bilayer (Figure 1b). The typical characteristics of the solar cells assembled using these HTL materials and non-exposed perovskite films are listed in Table 1. Note that while the efficiencies of the devices comprising PEDOT:PSS and NiO_x were not high (10-12%) due to intrinsic properties of the used charge transport interlayers, PCE of the best cells fabricated using PTAA as a hole-transport material approached almost 18%, which is an appreciably high value for perovskite solar cells assembled in p-i-n configuration.

Since we were not interested in the top electrode corrosion effects, we investigated the stability of the multilayered p-i-n stacks without top electrodes. Samples were subjected to light soaking with different exposure periods and the device structures were completed after aging simply by evaporation of top contacts (Figure 1a). In the *scenario 1*, light soaking induced certain aging effects in all functional layers of the devices with expect for top electrodes and top electrode/ETL interface, which were provided to be fresh due to their deposition after the aging step. Rapid decay of the solar cell efficiency in that case can be assigned to multiple possible degradation pathways or their combinations. In order to identify the real origins of the observed degradation effects, we have also realized the *scenario 2*, whose crucial stage was replacing the aged ETL represented by the fullerene derivative $PC_{61}BM$ with a freshly coated film of the same material (Figure 1a). This procedure, which we call below as "ETL refreshing", generates new ETL and ETL/perovskite interface while leaving the aged absorber layer and the perovskite/HTL interface.

Since the absorber layer is sufficiently stable and does not degrade significantly at the timescale of the experiment, the efficiency decay versus light exposure time for devices fabricated following *scenario 1* depends on the behavior of both top (ETL) and bottom (HTL) charge transport layers and interfaces. On the contrary, the degradation of the solar cells fabricated following *scenario 2* is associated mainly with HTL and HTL/perovskite interface behavior, while the ETL is provided fresh and should not affect the device performance. Thus, comparing the degradation kinetics of the devices fabricated following scenarios 1 and 2 and using identical samples allows us to decouple the aging effects induced at ETL/perovskite and HTL/perovskite interfaces.

The spectacular difference in the photovoltaic performance of the devices exposed to light soaking for 25 h and then processed following different scenarios is illustrated in Figure 2 for the samples assembled using PEDOT:PSS as HTL. The devices prepared following scenario 1 showed very low photovoltaic performance (V_{OC}~0.24V, J_{SC}~2mA cm^{-2}, FF~36% and PCE~0.3%,) and severely reduced external quantum efficiency (EQE), which reflected a massive light-induced degradation. This result is consistent with our previous reports showing

that the chemical interaction of MAI with the fullerene-based ETL ($PC_{61}BM$) causes rapid aging of the ITO/PEDOT:PSS/$MAPbI_3$/$PC_{61}BM$/Ag p-i-n solar cells[1].

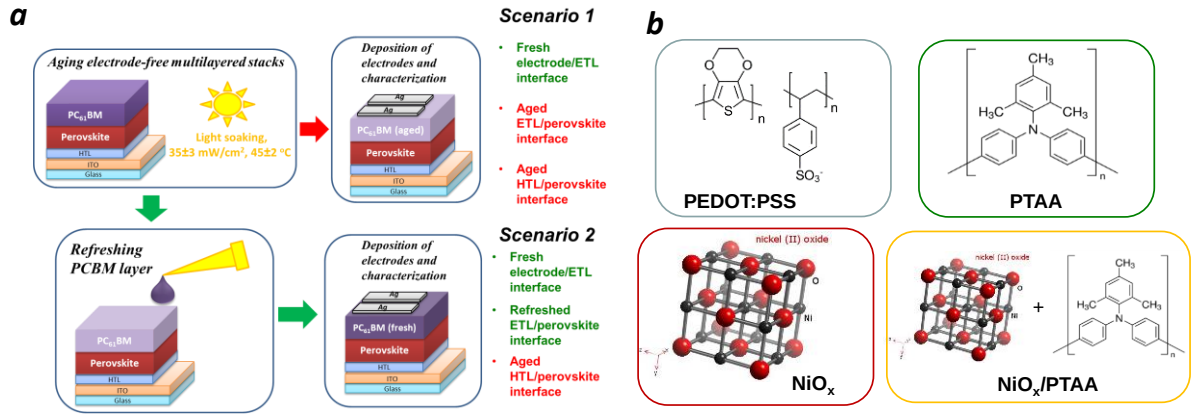

Figure 1 The general methodology of the performed experiments (a) and structural representation of the used model HTL materials (b).

Table 1 Efficiencies of the ITO/HTL/$MAPbI_3$/$PC_{61}BM$/Mg/Ag devices (perovskite films not exposed to light) extracted from reverse *J*-V scans at 10 mV/s voltage sweeping rate.*

HTL	V_{OC} (V)	J_{SC} (mA cm^{-2})	FF (%)	PCE (%)
PEDOT	0.91±0.04 (0.96)	13.0±0.5 (13.4)	78.0±2.0 (80.0)	9.3±0.6 (10.3)
PTAA	1.08±0.01 (1.09)	20.9±0.9 (22.0)	73.0±2.0 (74.0)	16.6±0.7 (17.9)
NiO_x	0.98± 0.01 (1.0)	15.9±0.9 (16.4)	69.0±7.0 (75.0)	10.7±1.1 (12.4)
NiO_x/PTAA	1.06±0.02 (1.08)	18.7±0.8 (19.4)	73.0±2.0 (72.0)	14.4±0.5 (15.2)

* - the data are given in the format "average ± deviation (champion cell parameter)"

Indeed, the devices fabricated following scenario 2 with refreshed ETL showed PCE~8%, EQE>60% and retained ~80% of the original performance of the solar cells fabricated using fresh films non-exposed to light. Thus, the obtained results confirm that $PC_{61}BM$/$MAPbI_3$ interface is mostly responsible for the observed degradation of the stacks under light exposure, while the PEDOT:PSS/$MAPbI_3$ interface provides just a minor contribution at this time scale (25 h).

Figure 3 shows an overview of the long-term aging kinetics of the samples incorporating different HTLs. The devices processed following *scenario 1* showed a comparably fast decay of the photovoltaic performance regardless the used HTL materials thus pointing to the fact that ETL is controlling their degradation. Such behavior is consistent with the reported previously mechanism implying that $PC_{61}BM$/$MAPbI_3$ interface is degrading under illumination due to liberation of MAI and its accumulation in the $PC_{61}BM$ layer[2].

[1] https://www.nrel.gov/pv/cell-efficiency.html
[2] A.F. Akbulatov, P.A. Troshin et al. *Adv. Energy Mater.* 7 (2017) 1700476

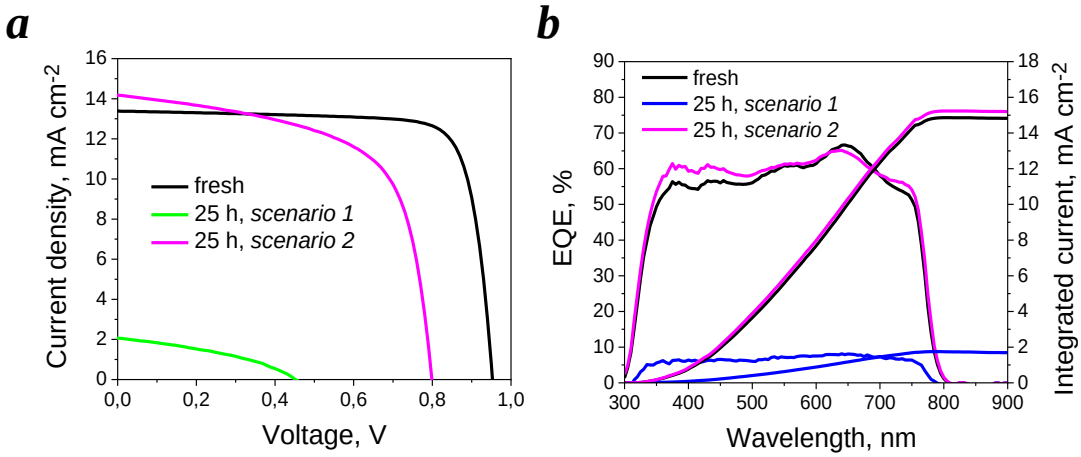

Figure 2 Impact of 25 h light exposure on the *J-V* characteristics (a) and EQE spectra (b) of the ITO/PEDOT:PSS/$MAPbI_3$/$PC_{61}BM$/Ag devices processed following scenarios 1 and 2.

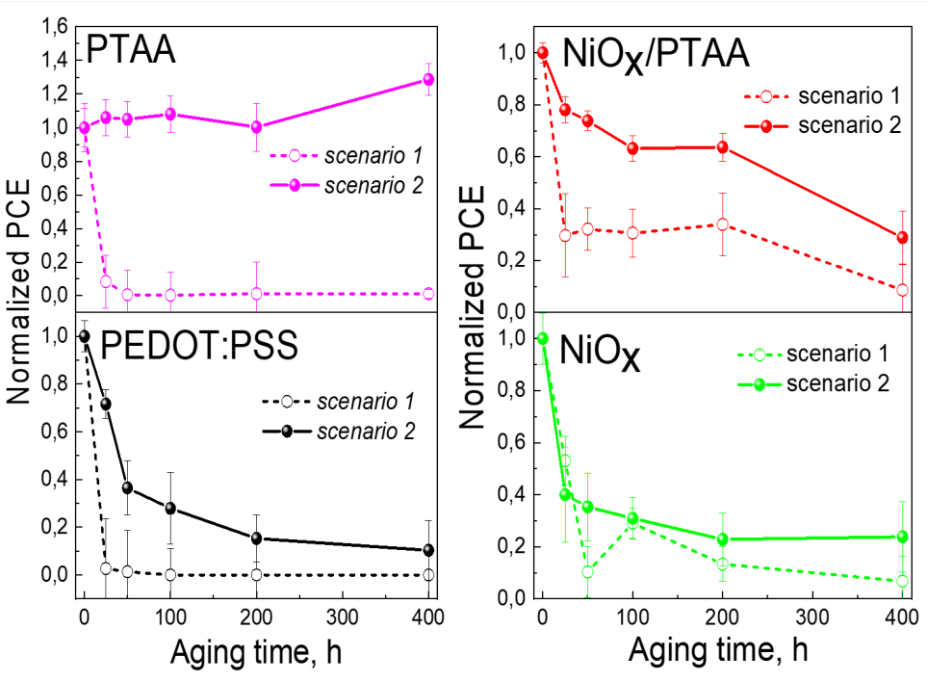

Figure 3 The aging kinetics of the samples assembled with PTAA, NiO_x/PTAA, PEDOT:PSS, and NiO_x as HTL materials under continuous white light soaking (35±3 mW/cm^2, 45±2 ^{o}C).

The obtained results support the previously made conclusion that the interface between $MAPbI_3$ and $PC_{61}BM$ is intrinsically unstable[3]. However, there are some examples of stable p-i-n perovskite solar cells with $MAPbI_3$/$PC_{61}BM$ interface reported in the literature[4,5,6]. This apparent contradiction might be explained by the realization of certain interface stabilization mechanisms, which still need to be thoroughly explored and understood.

[3] A.F. Akbulatov, P.A. Troshin et al. *Adv. Energy Mater.* 7 (2017) 1700476.
[4] K.O. Brinkmann, T. Riedl et al. *Nat. Commun.* 8 (2017) 1–9.
[5] J. Zhao, T. Riedl et al. *Adv. Energy Mater.* 7 (2017) 1602599.
[6] S. Wu, W. Chen et al. *Nat. Commun.* 10 (2019) 1–11.

The solar cells assembled with the refreshed ETL according to *scenario 2* showed spectacular different aging behavior depending on the used HTL material (Figure 3). The least stable were the samples incorporating PEDOT:PSS or NiO_x, which showed >70% decay of the photovoltaic performance within 400 h of light exposure. In contrast, the most stable interface was provided by the polymeric hole transport material PTAA, which allowed to maintain ~100% of the initial photovoltaic performance after 400 h of light exposure. This result confirms that the perovskite layer is sufficiently stable when sandwiched between two appropriate charge transport layers, e.g. PTAA and $PC_{61}BM$. Indeed, we showed recently that $PC_{61}BM$ coating prevents bulk degradation of $MAPbI_3$ under light exposure for >1000 h, while the aforementioned MAI to ETL diffusion pathway is realized only within the $MAPbI_3/PC_{61}BM$ interface[7]. Therefore, the decay in the photovoltaic performance of the samples processed following *scenario 2* can be entirely assigned to the degradation of the $HTL/MAPbI_3$ interfaces. It is notable that depositing PTAA as a passivation coating atop NiO_x, which appears to be quite aggressive with respect to the perovskite, slows down significantly the aging kinetics. However, the degradation of the samples cannot be prevented completely since PTAA coating is too thin (~20 nm) to block efficiently thick and rough film of NiO_x nanoparticles.

To summarize, we developed an efficient methodology for the investigation of interface degradation effects in p-i-n perovskite solar cells and decoupling the contributions of ETL/perovskite and perovskite/HTL junctions to the overall device aging kinetics. This approach opens wide opportunities for extensive screening of different HTL and ETL materials and comparing the stability of their interfaces with the absorber materials incorporated in various perovskite solar cell architectures. We showed, in particular, that PEDOT:PSS and NiO_x are not suitable HTL materials due to the aggressive chemistry occurring at their interfaces with hybrid lead halide perovskites as revealed by ToF SIMS analysis. In contrast, polymeric arylamine PTAA forms a very stable interface with complex lead halides and hence represents a highly promising hole-transport material. We believe that systematic application of the proposed here approach will strongly facilitate the development of stable interfaces for efficient and durable perovskite photovoltaics.

The 3rd chapter is entitled "Fullerene Derivatives as an Efficient and Stable Transport Layer for Inverted Perovskite Solar Cells". In this chapter, a systematic study of a family of structurally similar fullerene derivatives as electron transport layer (ETL) materials for p-i-n perovskite solar cells is presented.

Fullerene derivatives F1–F4 represent methanofullerenes and possess cyclopropane rings attached to the carbon cage with phenyl moiety as one of the substituent, which makes them similar to the reference $PC_{61}BM$ material as shown in Figure 4. Furthermore, the compounds F1–F3 can be considered as longer chain homologs of $PC_{61}BM$ because they represent propyl, butyl, and hexyl esters of phenyl-C_{61}-butyric acid, respectively. Compound F4 possesses no ester group in its molecular framework and, therefore, represents the least polar material in the series of F1–F4 and $PC_{61}BM$. Synthesis of F1–F4 was straightforward and

[7] A.G. Boldyreva, P.A. Troshin et al. *Sustain. Energy Fuels.* 3 (2019) 2705–2716.

based on the previously reported reactions of C_{60} with the corresponding tosylhydrazones promoted by sodium methylate and pyridine base system[8].

Fullerene derivatives F1–F4 were integrated as ETL materials in p-i-n PSCs with the architecture shown schematically in Figure 4.

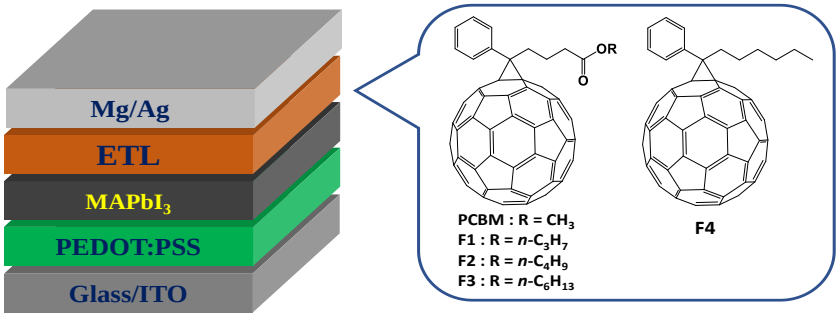

Figure 4 Molecular structures of the investigated fullerene derivatives F1–F4 and schematic layout of the used p-i-n solar cell architecture.

The *J*–*V* characteristics of the PSCs obtained under simulated AM1.5G illumination (100 mW cm^{-2}) while sweeping the voltage in forward and reverse directions are shown in Figure 5, whereas the device performance parameters are summarized in Table 2. The reference cells using conventional $PC_{61}BM$ as ETL material delivered the PCE of 14.6% with V_{OC} of 0.95 V, J_{SC} of 20.3 $mAcm^{-2}$, and FF of 79%. A comparable PCE of 14.6% was obtained for solar cells using F4 as ETL, though in combination with somewhat lower V_{OC} of 0.90 V. Fullerene derivatives F1, F2, and F3 provided lower PCEs of 11.4%, 12.3%, and 13.0%, respectively, due to slightly decreased J_{SC}, V_{OC}, and in some cases also FF. The current densities obtained from *J*–*V* measurements were reconfirmed by integration of external quantum efficiency (EQE) spectra against the reference AM1.5G solar spectrum (Figure 5f). The obtained in such way "integrated" current densities were 17.7 (F1), 18.1 (F2), 17.4 (F3) 18.9 (F4), and 18.3 ($PC_{61}BM$) mA cm^{-2}, thus matching well the values extracted from *J*–*V* curves.

We emphasize that the achieved PCEs of 11.4%–14.6% are among the best reported for PSCs assembled using PEDOT:PSS as a HTL, whereas the application of more promising materials such as polytriarylamine (PTAA) delivers improved efficiencies of up to 17%–19% while using F1–F4. Nevertheless, we intentionally performed a systematic study for devices incorporating PEDOT:PSS as a bottom hole-selective interlayer because it is hygroscopic and promotes actively ambient degradation of PSCs via the hydration pathway. As it is discussed below, some of the designed fullerene-based ETL can successfully mitigate moisture-induced degradation of PSCs in PEDOT:PSS-based p-i-n architecture and, therefore, should deliver even better performances in devices assembled with alternative less hygroscopic HTLs.

An important part of this study was related to the investigation of the ambient stability of nonencapsulated PSCs with different fullerene-based ETLs. It is known that lead halide perovskites, particularly $MAPbI_3$, undergo facile hydrolysis when exposed to moisture. The moisture-induced perovskite decomposition becomes the most severe in the case of using hydrophilic charge transport layers, particularly, PEDOT:PSS, which was intentionally

[8] J.C. Hummelen, C.L. Wilkins et al. *J. Org. Chem.* 60 (1995) 532–538.

selected as a hole-selective layer for our p-i-n devices (Figure 4). Initially, some stoichiometric hydrates are formed, whereas, at the final stage, only the phases of lead iodide and hydrated MAI can be detected in the system[9,10].

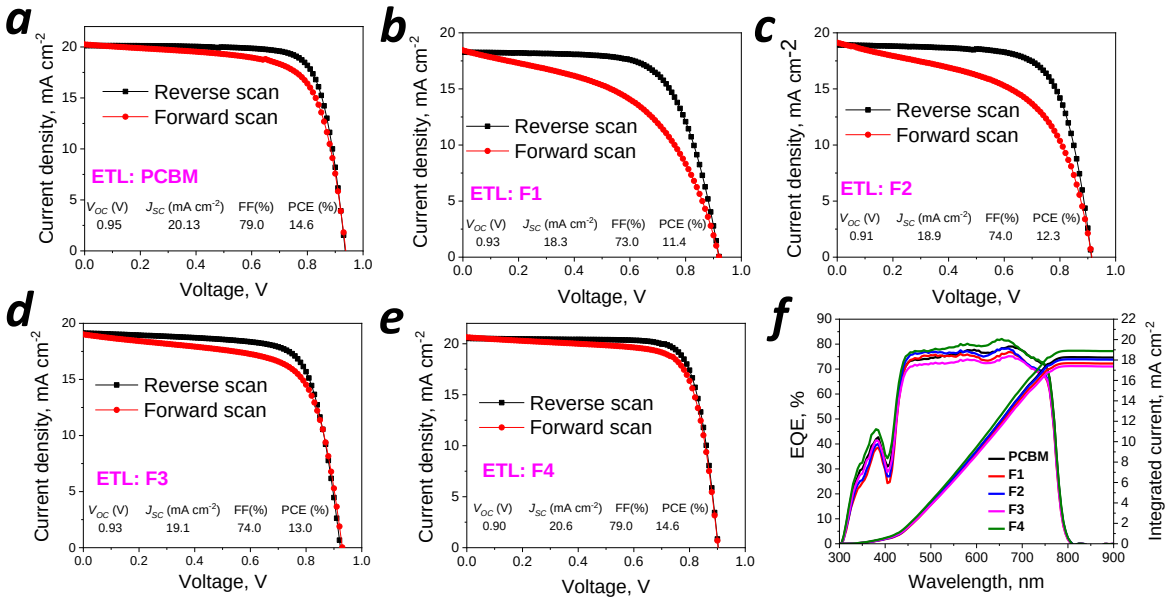

Figure 5 *J-V* curves measured in forward and reverse directions at a scan rate of 10 mV s^{-1} for p-i-n perovskite solar cells assembled with different ETLs: $PC_{61}BM$ (a), **F1** (b), **F2** (c), **F3** (d), **F4** (e), and (f) EQE spectra of PSCs using different fullerene-based ETL materials.

Table 2 Characteristics of PSCs with different fullerene-based ETLs.

ETL material	V_{OC} (V)	J_{SC} (mA cm^{-2})	FF (%)	PCE (%)
$PC_{61}BM$	0.94 ± 0.08	18.9 ± 1.4	72 ± 7	12.7 ± 1.2
	(0.95)	(20.3)	(79)	(14.6)
F1	0.92 ± 0.01	17.4 ± 1.3	68 ± 4	10.7 ± 0.8
	(0.93)	(18.3)	(73)	(11.4)
F2	0.91 ± 0.07	17.6 ± 1.2	71 ± 2	11.4 ± 0.8
	(0.91)	(18.9)	(74)	(12.3)
F3	0.91 ± 0.01	18.5 ± 1.3	68 ± 5	11.5 ± 0.9
	(0.93)	(19.1)	(74)	(13.0)
F4	0.88 ± 0.02	19.5 ± 1	71 ± 5	12.3 ± 1.4
	(0.90)	(20.6)	(79)	(14.6)

Average values for a batch of 16 devices are provided, while characteristics of the champion devices are shown in brackets.

Though the commercial PSCs are supposed to be well-encapsulated, their economically viable production apparently should be performed by coating all functional layers and, finally, sealing the devices in the air. Therefore, some limited exposure of the devices to ambient air is practically unavoidable.

[9] G.E. Eperon, H.J. Snaith et al. *ACS Nano*. 9 (2015) 9380–9393.
[10] A.M.A. Leguy, P.R.F. Barnes et al. *Chem. Mater.* 27 (2015) 3397–3407.

To assess the ambient stability of the fabricated PSCs, we continuously kept them in the air with a relative humidity of 30%–40% without intentional light exposure. The cells were periodically characterized by measuring their J–V characteristics and EQE spectra. Figure 6 shows the evolution of the normalized PSCs performance within 800 h of air exposure. It is seen that the solar cells using $PC_{61}BM$ and F4 as ETLs demonstrate the fastest degradation: PCE drops below 10% of the initial value within less than 100 h of exposure. PSCs assembled with ETLs based on F2 and particularly F3 demonstrated superior stability maintaining, respectively, ca. 30% and 50% of the initial efficiency after 100 h in ambient atmosphere. Most remarkably, the devices comprising F1 as ETL showed virtually no decay in the performance within the first 100 h. Moreover, these solar cells retained ≈90% of the initial performance after they were exposed to ambient air for 800 h.

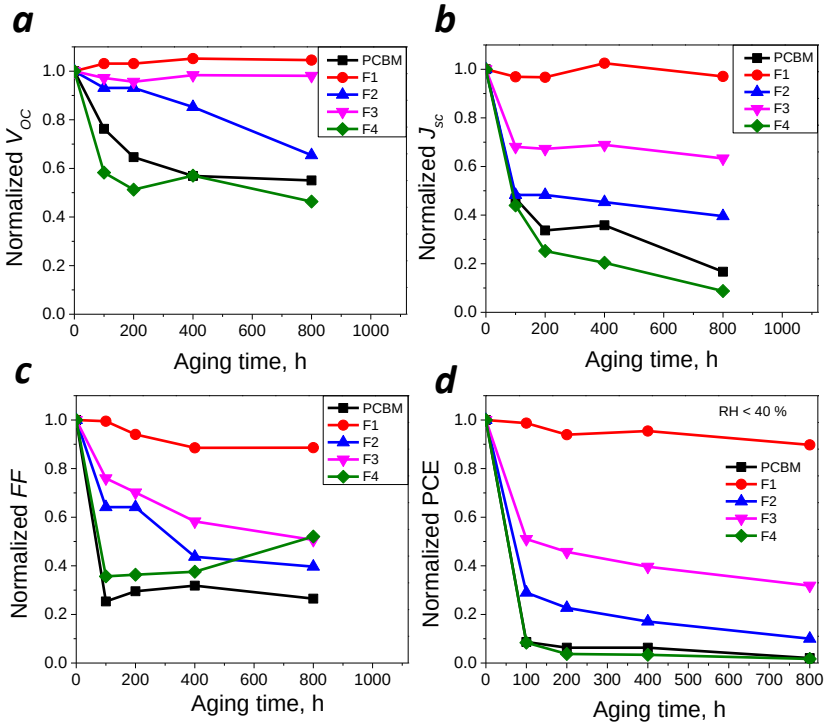

Figure 6 Evolution of the normalized parameters of p-i-n PSCs assembled with different fullerene-based ETLs.

To summarize, we explored a family of four different fullerene derivatives as ETL materials for p-i-n PSCs. It was shown that all designed compounds form high-quality coatings above the perovskite films without any detectable voids or pinholes. PSCs comprising fullerene-based ETLs F1–F4 and the reference $PC_{61}BM$ demonstrated comparable power conversion efficiencies, whereas their ambient stability was very different. The devices comprising reference $PC_{61}BM$ degraded almost completely within less than 100 h of air exposure. On the contrary, the solar cells assembled with the best-performing ETL material F1 maintained more than 90% of the initial efficiency after they spent 800 h under ambient atmosphere conditions (RH 30%–40%). The shown impressive ambient stability of PSCs induced by the fullerene derivative F1 applied as ETL was attributed to its optimal molecular architecture with the side chains filling the gaps between the fullerene spheres, thus preventing the diffusion of oxygen and moisture inside the device. The demonstrated effect of molecular

engineering paves a way toward a substantial improvement in the isolation characteristics of the fullerene-based ETLs, thus leading to increased operation lifetimes of perovskite photovoltaics.

The 4th chapter is entitled "Using conjugated polymers and oligomers as ETL materials for Perovskite Solar Cells". In this chapter, the conjugated polymer P1 based on pyrrolo[3,4-c]pyrrole-1,4-dione was explored as ETL material for PSCs alone or in composites with the fullerene derivatives (**Figure 7**). The conjugated polymer **P1** showed a high molecular weight of 162 kDa and a relatively low polydispersity index of 2.0, as well as a good solubility in organic solvents such as toluene, chlorobenzene and 1,2-dichlorobenzene.

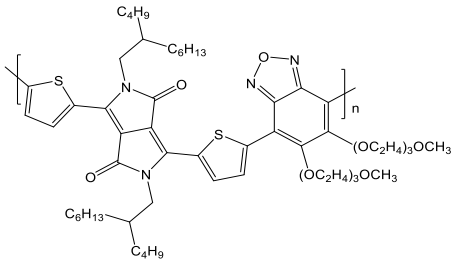

Figure 7 Molecular structure of conjugated polymer **P1**.

PSCs were fabricated in ITO/HTL/perovskite/ETL/Mg/Ag p-i-n configuration (**Figure 8**), where $PC_{61}BM$, **P1** or **P1**:$PC_{61}BM$ blend were used as ETL materials. The hybrid HTL consists of PTAA deposited on NiO_x, followed by the perovskite $Cs_{0.12}FA_{0.88}PbI_3$ as absorber. However, a pristine PTAA layer was used as HTL in $MAPbI_3$-based perovskite solar cells. The open-circuit voltage (V_{OC}), short-circuit current density (J_{SC}), fill factor (FF), and PCE of the optimized devices are presented in **Table 3**.

Figure 8 shows that polymer **P1** and, in particular, **P1**:$PC_{61}BM$ blend, delivered comparable performances to the reference devices with the pristine $PC_{61}BM$, which is a benchmark ETL material for p-i-n perovskite solar cells. The integration of the EQE spectra over the reference AM1.5G solar spectrum confirmed the values of the short-circuit current densities derived from *J*-V measurements. The open-circuit voltages were practically the same for solar cells assembled with all three types of ETL materials. However, the slope of the *J*-V curve near the open circuit point increases while going from pure $PC_{61}BM$ to pure **P1**, which indicates a notable increase in series resistance in the devices incorporating **P1**. The increase in the series resistance leads to a decrease in the device FF from 77% to 62%, which consequently lowers the average solar cell efficiency from 16.7% to 12.8%. Therefore, there is substantial room for further improvements by optimizing the structure of **P1** to improve its charge transport properties and prevent the extraction of holes from the absorber layer and the associated recombination losses.

At the next stage of this work, we investigated the operational stability of perovskite solar cells assembled using different ETL materials. The non-encapsulated PSCs with $Cs_{0.12}FA_{0.88}PbI_3$ absorber layer were subjected to continuous light soaking (metal-halide lamps, incident power 30±3 mW cm^{-2}, 45±2 °C) for 1200 hours in an inert nitrogen atmosphere using a special home-made setup integrated into an MBraun glove box. The efficiency of the reference devices using $PC_{61}BM$ as ETL dropped by 45% within the first 100 h of aging (**Figure 9)**.

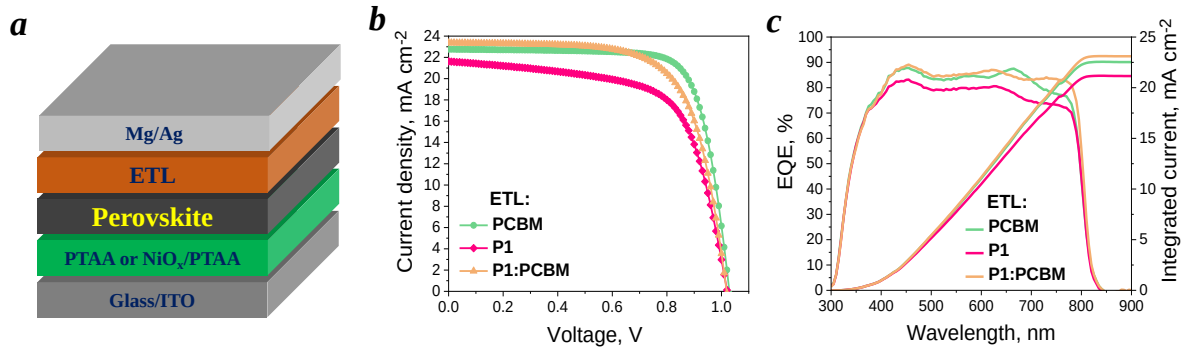

Figure 8 Schematic layout of perovskite solar cells architecture (a), *J*–V characteristics (b) and EQE spectra (c) of ITO/NiO_x/PTAA/$Cs_{0.12}FA_{0.88}PbI_3$/ETL/Mg/Ag PSCs assembled with different ETL materials.

Table 3 The performance parameters of perovskite solar cells assembled with different ETLs*

Perovskite	ETL	Scan direction	V_{OC} [V]	J_{SC} [mA cm^{-2}]	FF [%]	PCE [%]
$Cs_{0.12}FA_{0.88}PbI_3$	**$PC_{61}BM$**	Forward	1.01 ± 0.01 (1.02)	21.5 ± 0.8 (22.7)	76.0 ± 1.3 (75.6)	16.4 ± 0.8 (17.6)
		Reverse	1.01 ± 0.02 (1.03)	21.5 ± 0.8 (22.7)	77.0 ± 1.6 (76.0)	16.7 ± 0.8 (17.8)
	P1:$PC_{61}BM$	Forward	1.0 ± 0.02 (1.0)	22.3 ± 1.2 (23.4)	59.5 ± 1.8 (60.0)	13.1 ± 0.7 (13.8)
		Reverse	1.01 ± 0.01 (1.02)	22.2 ± 1.3 (23.4)	67.0 ± 2.2 (68.9)	15.0 ± 0.7 (16.4)
	P1	Forward	0.98 ± 0.02 (1.01)	20.4 ± 1.2 (21.9)	48.4 ± 5.0 (56.0)	9.7 ± 1.4 (12.4)
		Reverse	1.0 ± 0.02 (1.02)	20.7 ± 1.0 (21.6)	62.0 ± 3.0 (65.3)	12.8 ± 1.0 (14.4)
$MAPbI_3$	**$PC_{61}BM$**	Forward	1.08 ±0.02 (1.1)	19.6 ± 1.0 (20.8)	70.3 ± 2.6 (73.0)	15.0 ± 1.4 (16.8)
		Reverse	1.1 ± 0.01 (1.11)	19.6 ± 1.0 (20.7)	71.9 ± 2.4 (74.4)	15.5 ± 1.3 (17.2)
	P1	Forward	1.02 ± 0.02 (1.04)	18.4 ± 1.0 (18.8)	55.0 ± 2.4 (59.0)	10.2 ± 0.9 (11.5)
		Reverse	1.05 ± 0.01 (1.06)	18.5 ± 0.5 (18.4)	64.0 ± 2.4 (67.4)	12.5 ± 0.5 (13.2)

* The standard deviation was calculated for a batch of 16 cells tested under forward and reverse scan directions. Values in parentheses are for the best-performing device.

The PSCs incorporating **P1** as ETL showed even faster degradation with about 55% loss in PCE after 100 h. On the contrary, using the composite **P1**:$PC_{61}BM$ as ETL provided

remarkably improved stability: the devices lost less than 10% of the initial PCE after 100 h of aging and retained ca. 70% of the original efficiency after 1200 h of continuous light soaking. To the best of our knowledge, this is the longest lifetime demonstrated for p-i-n perovskite solar cells assembled using fully organic ETL materials.

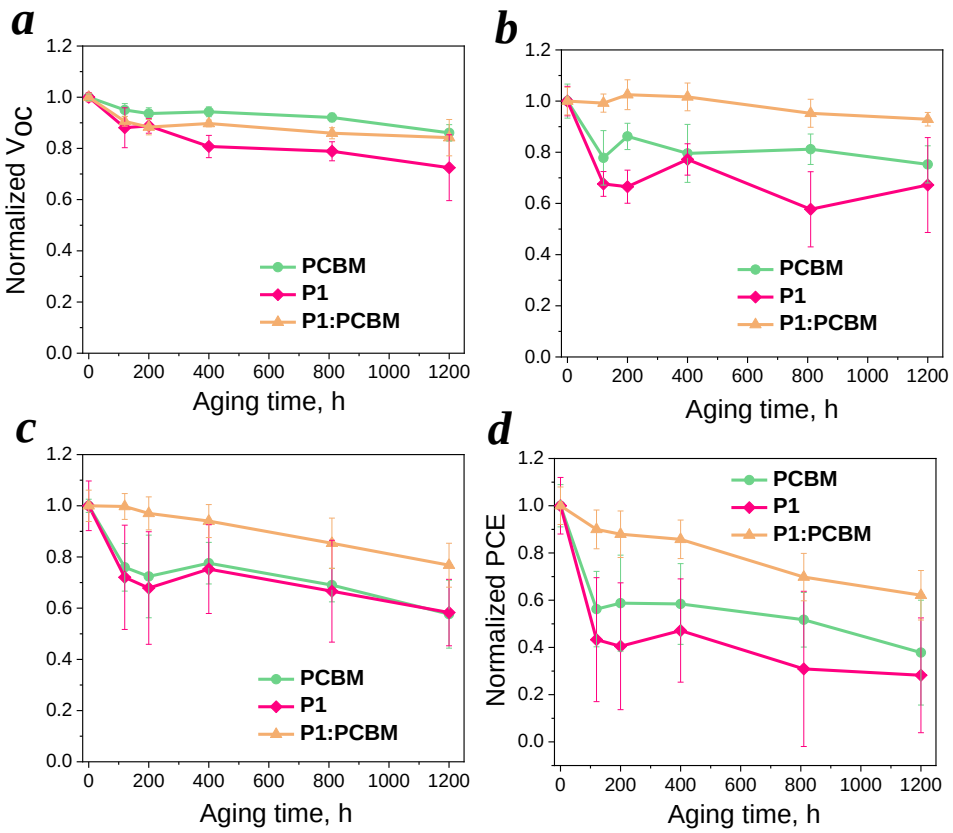

Figure 9 Operational stability of the ITO/NiO_x/PTAA/$Cs_{0.12}FA_{0.88}PbI_3$/ETL/Mg/Ag perovskite solar cells using **P1** (violet), **P1**:$PC_{61}BM$ (orange) and $PC_{61}BM$ (green) as ETL materials (30±3 mW cm^{-2}, 45±2 °C, nitrogen atmosphere). Evolution of the normalized open circuit voltage (a), short circuit current density (b), FF (c) and power conversion efficiency (d) is shown.

To summarize, a new conjugated polymer with pyrrolo[3,4-c]pyrrole-1,4-dione and 2,1,3-benzooxadiazole acceptor blocks was introduced as electron transport material in perovskite solar cells. Owing to the optimal LUMO energy of -4.1 eV, well matching the perovskite conduction band, **P1** demonstrated decent efficiencies of 13-14% when used as an electron transport layer in p-i-n PSCs. The devices assembled with **P1** as ETL material showed increased series resistance leading to reduced FF and PCE values as compared to the reference cells using $PC_{61}BM$ as ETL. Therefore, better performances seem to be reachable via further optimization of the molecular structure of **P1** with a primary focus on improving its charge transport properties. The 1:1 w/w blend of polymer **P1** with $PC_{61}BM$ provided increased device efficiency reaching 16.4% and, most importantly, an impressive improvement in operational stability of PSCs. Indeed, the optimized devices retained ~70% of the initial PCE after 1200 h of continuous light exposure. The obtained results feature the potential of the rational design of polymeric ETL materials for the development of efficient and stable perovskite solar cells.

The 5th chapter is entitled "Tungsten oxide as a promising ETL material enabling high efficiency and record-breaking operational stability of p-i-n PSCs". In this chapter, we apply for the first time tungsten oxide WO_X as electron-transport material for p-i-n perovskite solar cells using thermal evaporation of WO_3 in vacuum.

We fabricated devices with the ITO/PTAA/$MAPbI_3$/WO_X/Al(Ag) architecture as shown in figure 10a. The energy level alignment for the used materials[11] is shown in figure 10b. First, we optimized the thickness of ETL by depositing 10, 30, or 60 nm WO_X. Using the thinnest WO_X films (10 nm) provided low efficiency, which is apparently caused by incomplete $MAPbI_3$ film coverage. The thickest WO_X ETL layer (60 nm) also did not provide high efficiency due to the increased series resistance. However, using the optimal 30 nm thick WO_X deliverd the best device performances.

Figure 10c shows the *J–V* curves of the champion devices assembled with the reference $PC_{61}BM$ and WO_X (30 nm) ETLs measured in forward and reverse directions at a scan rate of 10 mV s^{-1}. The photovoltaic parameters of the devices are summarized in table 4. Using $PC_{61}BM$ as a reference ETL we obtained PCE of 18.5% , V_{OC} of 1.11 V, J_{SC} of 21.4 mA cm^{-2}, and FF of 78.0 % under reverse scan. The champion device with WO_X (30 nm) used as ETL delivered PCE of 15.5% with V_{OC} of 0.96 V, J_{SC} of 21.6 mA cm^{-2}, and FF of 74.7% as extracted from the reverse J-V scan.

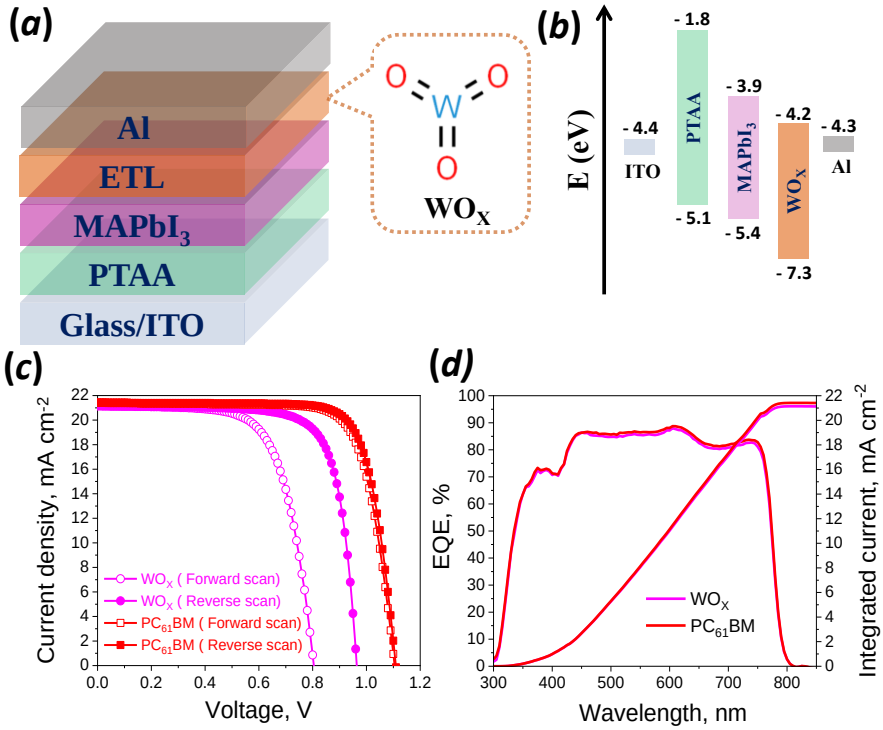

Figure 10 The performance of WO_x as ETL in p-i-n perovskite solar cells. (a) Schematic illustration of the ITO/PTAA/$MAPbI_3$/WO_X/Al architecture. (b) Energy level diagram for all the components of the fabricated devices. (c) J–V characteristics for the champion devices using WO_X (30 nm) and $PC_{61}BM$ ETLs under the simulated AM1.5G illumination conditions measured with a scan rate of 10 mV s^{-1}. (d) EQE spectra and integrated current densities for the corresponding devices.

[11] M. Ye, Z. Lin et al. *J. Phys. D: Appl. Phys.* 50 (2017) 373002.

EQE spectra of the devices assembled with WO_X and $PC_{61}BM$ ETLs are presented in Figure 10d. The integrated J_{SC} values obtained from the EQE spectra were 21.1 and 21.3 mA cm^{-2} for devices with WO_X and $PC_{61}BM$ ETLs, respectively, which are in a good agreement with the J_{SC} values extracted directly from the *J–V* curves.

Thus, we successfully integrated WO_X as ETL material for p-i-n perovskite solar cells. However, the devices using WO_X as ETL show poor V_{OC} and a big hysteresis in J-V characteristics due to the unbalanced charge extraction and suspected recombination losses at the $MAPbI_3/WO_X$ interface. These issues might be solved by using a proper interlayer between $MAPbI_3$ and WO_X layers.

First, we investigated C_{60} as an interlayer between $MAPbI_3$ and WO_X. We fabricated devices based on ITO/PTAA/$MAPbI_3$/C_{60}/WO_X (30nm)/Al architecture assembled with a varied thickness of C_{60} interlayer (5, 10, and 15 nm) deposited by thermal evaporation. The reference cells with WO_X (30 nm) as a single-component ETL yielded PCE of 14.1% with a V_{OC} of 0.98 V, a J_{SC} of 19.5 mA cm^{-2}, and FF of 73.6 % under reverse scan direction. Inserting C_{60} interlayer between $MAPbI_3$ and WO_X (30 nm) led to a spectacular improvement in V_{OC} and decreased hysteresis. Using the optimal thickness of C_{60} (10 nm) and WO_X (30 nm) yielded PCE of 16.2% with V_{OC} of 1.06 V, a J_{SC} of 20.7 mA cm^{-2}, and FF of 73.4% as extracted from the reverse scan. Figure 11a shows the current-voltage (*J–V*) characteristics of the best devices with and without C_{60} (10 nm). Literature reports suggest that C_{60} enhances the extraction of electrons from the perovskite in p-i-n devices and suppresses the hysteresis by minimizing space charge accumulation at the interface[12,13].

At the next stage of the experiment, we for the first time utilized WO_X as a component of both HTL and ETL in inverted PSCs, which means that the same material (WO_X) plays two roles at the same time. We fabriciated devices in the ITO/**WO_X**/PTAA/$MAPbI_3$/C_{60}(10 nm)/**WO_X**(30 nm)/Al architecture with varied thickness of WO_X layer within the hybrid HTL (8 and 16 nm) deposited by thermal evaporation in the same way as in the case of WO_X ETL. Using WO_X as HTL enhanced V_{OC}, J_{SC}, and FF, leading to the PCE of 17.32%, V_{OC} of 1.04 V, J_{SC} of 21.6 mA cm^{-2}, and FF of 78.0% as shown in figure 11b. The combination of WO_X with PTAA enhanced the performance of the devices due to improved hole extraction. Also, using WO_X as HTL component provided a more efficient barrier between the ITO and the perovskite absorber layer, which could react with each other[14].

Table 4 Photovoltaic parameters of perovskite solar cells using WO_X and $PC_{61}BM$ as ETLs.

ETL	Scan direction	V_{OC} (V)	J_{SC} (mA cm^{-2})	FF (%)	PCE (%)	J_{cal} [a] (mA cm^{-2})
WO_X (30 nm)	FS	0.81	21.6	67.7	11.8	21.1
	RS	0.96	21.6	74.7	15.5	
$PC_{61}PM$	FS	1.10	21.4	76.7	18.1	21.3
	RS	1.11	21.4	78.0	18.5	

[a] The J_{cal} values were calculated from the EQE curves.

[12] X. Liu, G. Liao et al. *Electrochim. Acta*. 288 (2018) 115–125.
[13] D. Liu, R.R. Lunt et al. *ACS Nano.* 12 (2018) 876–883.
[14] S.Y. Luchkin, K.J. Stevenson et al. *ACS Appl. Mater. Interfaces*. 9 (2017) 33478–33483.

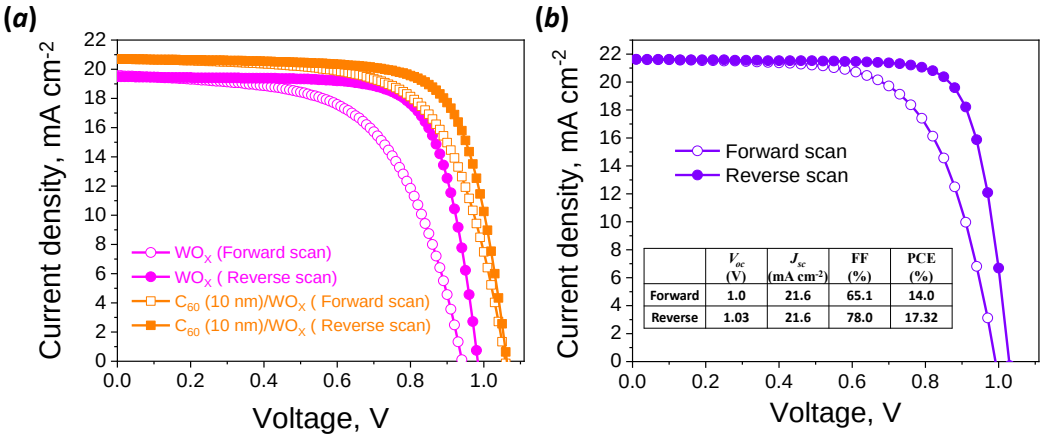

Figure 11 *J-V* curves for best devices with and without C_{60} (10 nm) interlayer (a). *J-V* curves for devices using optimal WO_X thickness (8 nm) within HTL (b).

Bathocuproine (BCP) is another material that is widely utilized to form bilayer ETLs in inverted PSCs. BCP has a deep HOMO energy level (−7.0 eV) and can act as an efficient hole-blocking layer in p-i-n PSCs. Using BCP might help to suppress the charge recombination at the ETL/top electrode interface. Therefore, we introduced 4 nm of BCP between WO_X and Al and this combination delivered PCE of 17.6% with significantly improved V_{OC} and J_{SC} as shown in figure 12a. Following the same strategy, we also used 4,7-diphenyl-1,10-phenanthroline (BPhen) as an interlayer between WO_X and Ag. Figure 12b shows that the device employing C_{60}/WO_X/BPhen as tricomponent ETL exhibited the enhanced PCE of 18.4% with a negligible hysteresis.

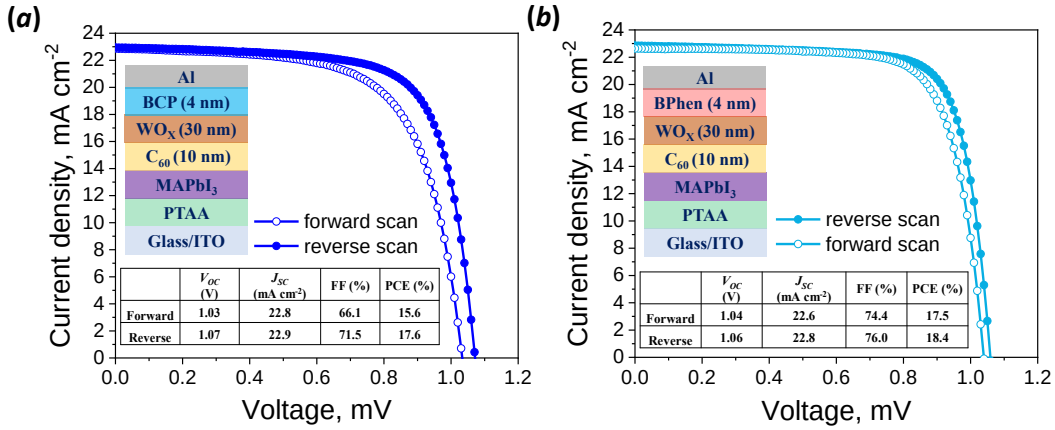

Figure 12 The current-voltage characteristics of the devices using triple-layer C_{60}/WO_X/BCP (a) and C_{60}/WO_X/BPhen (b) ETLs.

To date, the p-i-n devices demonstrate very limited lifetimes under continuous light soaking, which do not exceed 1000 h to the best of our best knowledge[15,16,17]. To explore the effect of WO_X ETL on the device stability, we performed aging tests for

[15] W. Chen, Z. He et al. *Adv. Mater.* 29 (2017).
[16] Y.H. Chiang, P. Chen et al. *J. Mater. Chem. A.* 5 (2017) 25485–25493.
[17] Y. Wu, L. Han et al. *Nat. Energy*. 1 (2016) 1–7.

ITO/PTAA/$MAPbI_3$/WO_X/Al and the reference ITO/PTAA/$MAPbI_3PC_{61}BM$/Al cells using continuous illumination with the light power of 70 mW cm^{-2} and the temperature of 55-60 °C.

The evolution of the normalized device parameters vs. aging time is presented in figure 13. The efficiency of the reference cells using $PC_{61}BM$ as ETL dropped dramatically from 16.6% to 0.34 % within 166 h of aging, which was accompanied by the massive degradation of J_{SC} and FF. In contrast, the devices using WO_X as ETL showed >85% retention of the initial performance under the same conditions. Furthermore, the WO_x-based cells maintain ≈65% of the starting PCE after 4600 h of aging due to the stabilized J_{SC} and FF. Thus, using WO_X as ETL enabled record-breaking operational stability of $MAPbI_3$-based p-i-n erovskite solar cells.

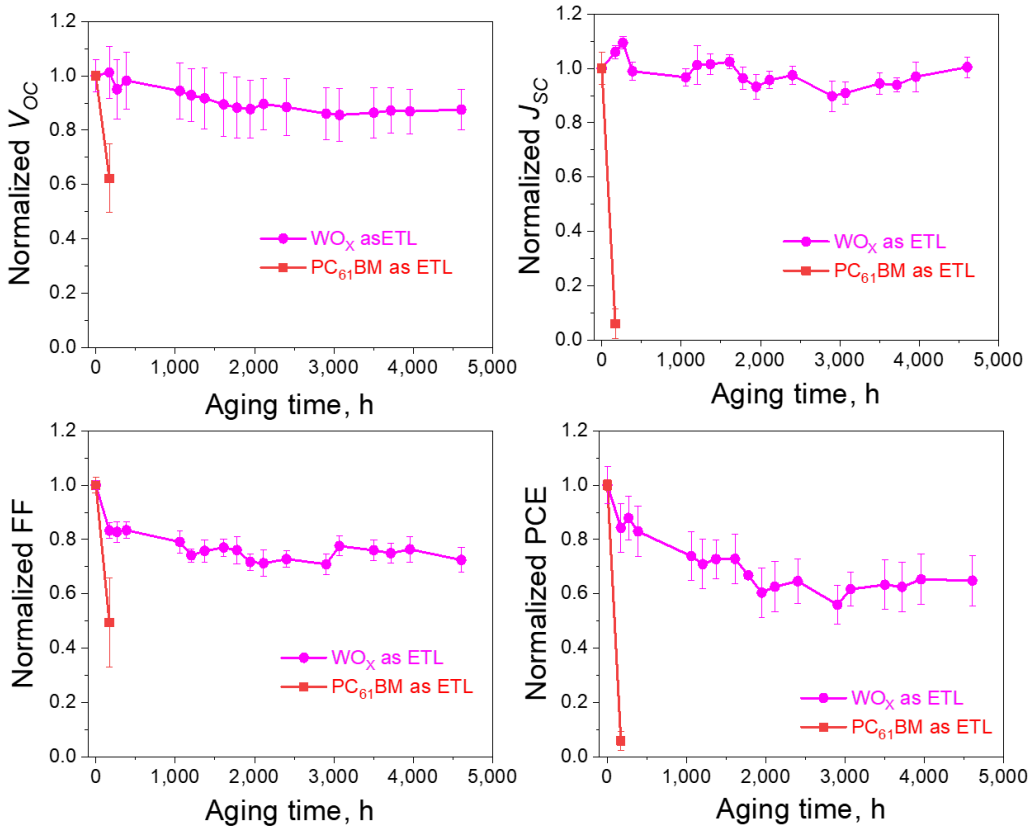

Figure 13 Operational stability of the ITO/PTAA/$MAPbI_3$/**ETL**/Al solar cell architectures using WO_X or $PC_{61}BM$ as ETLs under continuous light soaking (60 °C, 70 mW cm^{-2}).

Thus, for the first time we successfully integrated WO_X as ETL material in inverted PSCs. The solar cells with engineered ETL using WO_x as one of the components delivered high efficiency of 18.4% and reduced hysteresis. Most importantly, the devices using WO_X as ETL demonstrated record-breaking operational stability under continuous light soaking without encapsulation for 4600 h, which is the best result ever reported for p-i-n perovskite solar cells. The obtained data show that WO_X represents innovative ETL material for stable and efficient p-i-n perovskite solar cells.

Summary

In this thesis, systematic study of different types of ETL materials based on new fullerene derivatives, conjugated polymers and metal oxides is presented. The introduced novel materials and the developed experimental approaches resulted in improved efficiency and largely enhanced operational stability of p-i-n PSCs.

In particular, an efficient methodology was developed for the investigation of interface degradation effects in p-i-n perovskite solar cells (PSCs). The proposed approach allows one to decouple the contributions of ETL/perovskite and perovskite/HTL interfaces to the overall device aging kinetics.

A series of structurally similar fullerene derivatives were systematically studied as ETL materials in p-i-n PSCs. It was shown that even minor modifications of the molecular structure of the fullerene derivative have a strong impact on their electrical performance and, particularly, the ambient stability of the devices. Indeed, an optimally functionalized fullerene derivative applied as an ETL enables stable operation of perovskite solar cells when exposed to air for >800 h, which is manifested in retention of 90% of the original photovoltaic performance.

A novel pyrrolo[3,4-c]pyrrole-1,4-dione-based n-type conjugated polymer was investigated as an electron transport material for perovskite solar cells. By blending this polymer with the fullerene derivative $PC_{61}BM$ we achieved a decent power conversion efficiency of 16.4% in p-i-n perovskite solar cells using methylammonium-free $Cs_{0.12}FA_{0.88}PbI_3$ absorber in combination with the substantially improved operational stability of the devices.

Conjugated oligomeric compounds TBTBT and F4TBTBT ("T" - thiophene, "B" - benzothiadiazole) were studied as electron transport materials for p-i-n PSCs. The fabricated devices demonstrated a decent power conversion efficiency (PCE) of 10.5%, which was improved to 17.8% by inserting a thin $PC_{61}BM$ interlayer between the perovskite absorber layer and TBTBT-based ETL. The use of TBTBT as ETL enhanced the operational stability of perovskite solar cells as compared to the reference devices using the conventional fullerene derivative $PC_{61}BM$.

Tungsten oxide (WO_X) was integrated for the first time as electron-transport material for p-i-n PSCs. A high photovoltaic efficiency of up to 18.4% was achieved in combination with the record-breaking operational stability of the devices under continuous light soaking at a high temperature of 60 ^oC. Indeed, the $MAPbI_3$-based PSCs with WO_X electron-transport layer retained ~70% of their initial performance after 4600 h of aging under such harsh conditions, whereas the reference cell assembled with $PC_{61}BM$ degraded completely within 50 h.

Thus, the results presented in this thesis are expected to facilitate the transition of perovskite solar cells from research labs towards commercial production.

Author's publications on the dissertation topic

1.**M. Elnaggar**, M. Elshobaki, A. Mumyatov, S. Yu. Luchkin, K. J. Stevenson, P. A. Troshin, Molecular engineering of the fullerene-based electron transport layer materials for improving ambient stability of perovskite solar cells. RRL Solar, **2019**, 3, 1900223. **https://doi.org/10.1002/solr.201900223**

2. A. G. Boldyreva, A. F. Akbulatov, **M. Elnaggar**, S. Yu. Luchkin, A. V. Danilov, I. S. Zhidkov, O. R. Yamilova, Yu. S. Fedotov, S. I. Bredikhin, E. Z. Kurmaev, K. J. Stevenson, and P. A. Troshin. Impact of charge transport layers on photochemical stability of $MAPbI_3$ in thin films and perovskite solar cells, Sustainable Energy Fuels, **2019**, 3, 2705-2716. https://doi.org/10.1039/C9SE00493A

3.**M. Elnaggar**, A. G. Boldyreva, M. Elshobaki, S. A. Tsarev, Y. S. Fedotov, O. R. Yamilova, S. I. Bredikhin, K. J. Stevenson, S. M. Aldoshin and P. A. Troshin. Decoupling Contributions of Charge-Transport Interlayers to Light-Induced Degradation of p-i-n Perovskite Solar Cells. RRL Solar, **2020**, 4, 2000191. **https://doi.org/10.1002/solr.202000191**

4. **M. Elnaggar**, A. M. Gordeeva, A. V. Akkuratov, S. Yu. Luchkin, S. A. Tsarev, K. J. Stevenson, S. M. Aldoshin, P. A. Troshin. Improving Stability of Perovskite Solar Cells Using Fullerene-Polymer Composite Electron Transport Layer. Submitted, **2021**.

5. **M. Elnaggar**, S. M. Aldoshin, P. A. Troshin. Alternating Thiophene-Benzothiadiazole Oligomer as Electron Transport Material for Inverted Perovskite Solar Cells. Submitted, **2021**.

6. **M. Elnaggar**, S. M. Aldoshin, P. A. Troshin et al., Using Tungsten Oxide as ETL Material Enables High Efficiency and Long-Term Operational Stability of p-i-n Perovskite Solar Cells. Submitted, **2021**.